Self-Driving Capacitive Cantilevers for High-Frequency Atomic Force Microscopy

Self-driving capacitive cantilevers for high-frequency atomic force microscopy

Keith A. Brown,[a] Benjamin H. Yang, and R.M. Westervelt[b]

School of Engineering and Applied Sciences and Department of Physics,
Harvard University
Cambridge, Massachusetts 02138, USA

Abstract: We demonstrate a simple way to actuate an atomic force microscope cantilever at high frequencies by electrically driving a thin-film capacitor on its surface. Capacitive driving directly actuates the vibrational mode of the cantilever, removing the effects of unwanted mechanical modes present in conventional driving systems and removing the need for a drive piezoelectric. Practical vibration amplitudes are attainable at drive voltages < 5 V. We capacitively drive the first mechanical resonance of a tapping mode cantilever (243 kHz) and a high-frequency cantilever (1.5 MHz) with vibration amplitudes in agreement with our model of capacitive driving.

PACS numbers: 07.79.Lh, 85.85.+j

[a] Currently at Northwestern University

[b] Electronic mail: westervelt@seas.harvard.edu

A major trend in atomic force microscopy (AFM) and other cantilever-based microelectromechanical systems (MEMS) is to use cantilevers with higher resonance frequencies f_0 to allow for faster measurements and greater sensitivity. High-frequency measurements have been useful for ultrafast topographic scanning,[1] monitoring real-time dynamics of biological processes,[2,3] mechanical measurements through contact resonance,[4] and biodetection.[5,6] Conventional dynamic AFM uses cantilevers with $f_0 \sim 200$ kHz driven by a piezoelectric element on the holder.[7] The utility of conventional piezoelectric drive is diminished at high frequencies $f_0 \geq 1$ MHz because unwanted mechanical modes in the cantilever holder play a greater role.[8] Techniques have been developed to drive the cantilever directly in order to improve its coupling with the actuator. Laser illumination has been used to drive cantilevers through the photothermal effect,[9] and electrodes on the sample have been used to electrostatically actuate cantilevers.[10] Actuators have also been fabricated onto cantilevers to drive them directly, such as piezoelectrics,[11] Schottky diodes[12] and transistors.[13] Capacitors with air[14,15] and dielectric[16] gaps integrated with AFM cantilevers have previously been used to drive and sense deflections of cantilevers with low ($\leq$ 60 kHz for air gaps and $\sim$ 2 kHz for dielectric gaps) resonance frequencies.

In this paper, we demonstrate that capacitive driving is a simple and robust method for actuating cantilevers at high frequencies. We begin by describing how a driving force is created by a thin film capacitor on the surface of a cantilever. To compare their performances at different frequencies, capacitors are fabricated on conventional and high-frequency AFM cantilevers. Our measurements show that capacitively-driven cantilevers display improved drive fidelity over mechanical driving. High-frequency cantilevers show a dramatic improvement with capacitive driving because mechanical driving by a piezoelectric element is complicated by many spurious modes. We find that the magnitude of the vibration amplitude is in good agreement with a simple model of capacitive drive.

A thin-film capacitor fabricated on the surface of an AFM cantilever can be used to mechanically actuate the cantilever by applying a voltage V across the capacitor.[16] A rectangular cantilever of length L, width W, and thickness T is shown in Fig. 1(a). A capacitor with capacitance C is formed by the conducting cantilever and a metal layer deposited on its entire bottom surface separated by an insulator of thickness D and relative permittivity ε. When the

cantilever is deflected a distance z at its tip, the bending creates mechanical strain in the capacitor[17] which directly changes its dimensions and changes ε through electrostriction,[18] as shown in Fig. 1(b). Conversely, when a voltage V is applied across C, the dependence of C on z leads to an effective force F on the tip, which to first order in strain is:

$$F = \beta \frac{TW}{LD}\left(1 - \frac{\Delta\varepsilon}{\varepsilon}\right)\varepsilon\varepsilon_0 V^2, \tag{1}$$

where ε_0 is the permittivity of free space, and $\Delta\varepsilon = a_1\nu - a_2(1-2\nu)$ is the reduction in ε due to electrostriction, which depends on the Poisson's ratio ν, the shear electrostriction constant a_1, and the bulk electrostriction constant a_2.[18] We calculate $\Delta\varepsilon = 3.3$ for the material used below - low stress silicon nitride grown with plasma-enhanced chemical vapor deposition (PECVD) for which $\varepsilon = 5.5$[19] and $\nu = 0.21$.[20] The constant β depends on the cantilever shape, $\beta = 3/8$ for a rectangular cantilever and $\beta = 1/4$ for a triangular cantilever with base width W. The cantilever spring constant k also depends on the geometry of the cantilever.[21]

Electrostatic actuation by a capacitor is useful for driving cantilevers near their mechanical resonance. The vibration amplitude A of a cantilever in response to the capacitive force F from Eq. (1), when driven by an ac voltage near the cantilever's resonant frequency f_0 is:

$$A = \frac{F}{k}\left\{\left[1 - \left(\frac{f}{f_0}\right)^2\right]^2 + \left(\frac{f}{f_0 Q}\right)^2\right\}^{-1/2}, \tag{2}$$

where Q is the quality factor of the resonance. If the cantilever is capacitively driven with a voltage $V = V_{DC} + V_{AC}\sin(2\pi ft)$, the quadratic dependence of F on V from Eq. (1) indicates that there will be force contributions at dc, f, and $2f$. A robust driving force can be obtained by driving at half the resonant frequency with $f = f_0/2$.

Capacitive cantilevers are made using a fabrication protocol similar to our procedure for making coaxial AFM probes.[22,23] Conventional tapping mode (Arrow-NCPt, NanoAndMore AG) and high-frequency (Arrow-UHF, NanoAndMore AG) conducting AFM cantilevers are

chemically cleaned and mounted on a metal carrier. The cantilevers are coated with 25 nm of Ti using electron-beam evaporation (EE) for adhesion. PECVD is used to deposit a ~ 50 nm thick insulating layer of low-stress SiN_x on the cantilever. An additional ~ 2 μm insulating layer is deposited on the cantilever holder to make it mechanically and electrically robust. Finally, 30 nm of Ti and 50 nm of Au are deposited on the cantilevers by EE. AFM experiments are performed in a commercial system (MFP-3D, Asylum Research) with a custom tip holder that makes separate electrical contact to the top and bottom of the probe chip. A glass substrate is used to calibrate cantilever deflection, but all measurements are taken with the cantilever ~1 cm from the substrate.

Figure 2 shows a comparison of AFM cantilever response to capacitive and mechanical driving for a conventional tapping mode cantilever (f_0 = 243 kHz) and a high-frequency cantilever (f_0 = 1.5 MHz). The left column in Fig. 2 shows data taken with the tapping mode cantilever shown in Fig. 2(a), while the right column shows data taken with the high-frequency cantilever shown in Fig. 2(e). The principle mechanical resonance is found by observing the thermal noise spectra n_A, shown in Figs. 2(b) and 2(f). The resonances appear cleanly in n_A and are fit to the thermal vibration spectrum of the peak (Eq. (9) from ref. [24]) added in quadrature to white noise,[25] with results summarized in Table I. Figures 2(c) and 2(g) show the vibration amplitude A observed when mechanically driving the cantilevers with the piezoelectric element. The resonance peak for the tapping mode cantilever shows only a slight deviation from the fit, while A of the high-frequency cantilever is complicated by many spurious features that make it impossible to locate the true resonance peak. This deviation is due to the activation of unwanted modes of vibration between the piezoelectric drive source and the cantilever, which produces spurious modes through intermodulation distortion.

Figures 2(d) and 2(h) show high-quality capacitive driving of the tapping mode and high-frequency cantilevers, respectively. In both cases, the response is clean and fits Eq. (2) very well. The high level of agreement between A and the fit indicates that the vibrational mode is being driven with high fidelity. Capacitive driving is able to effectively avoid the spurious modes encountered with piezoelectric drive because it is directly attached to the cantilever. For the tapping mode cantilever, the fit indicates that f_0 = 243.2 kHz and Q = 533 ± 1 with drive voltages V_{DC} = 3 V and V_{AC} = 1 V. For the high-frequency cantilever, the fit gives f_0 = 1.526 MHz and Q

= 187 ± 3 with V_{DC} = 5 V and V_{AC} = 5 V. Both cantilevers show excellent agreement between the resonances measured in the capacitive drive response and n_A.

The vibration amplitude A found for capacitive drive is in good agreement with our model. Figures 3(a) and 3(b) show A *vs*. V_{AC} for a tapping mode and a high-frequency cantilever, respectively, both driven at $f = f_0/2$. Both curves are well-fit by $A = \alpha_{\text{exp}} V_{AC}^2$, where α_{exp} is the experimentally determined capacitive driving coefficient. Values of α_{exp} for two cantilevers are compared with the theoretically predicted capacitive driving coefficient α_{theory} in Table 1; α_{theory} is found by combining Eq. (1) with Eq. (2) using $f = f_0/2$ to find,

$$\alpha_{theory} = \frac{\beta}{2}\frac{Q}{k}\frac{TW}{LD}\left(1 - \frac{\Delta\varepsilon}{\varepsilon}\right)\varepsilon\varepsilon_0 . \tag{3}$$

Values of α_{theory} are calculated for the rectangular tapping mode and triangular high-frequency cantilevers using ε = 5.5 and $\Delta\varepsilon$ = 3.3 and the parameters given in Table I. Both cantilevers are in good agreement with the theory. The high-frequency cantilever is less ideal, possibly due to the thickness of the cantilever being similar to the thickness of the capacitor, resulting in deviations from behavior as an ideal beam.

Capacitive driving can in principle be used at high frequencies (above 1 GHz) and for driving higher vibrational or torsional modes. As sensitivity and bandwidth increase with cantilever resonance frequency,[6,26] it is important to consider the maximum frequency at which capacitive driving technique remains practical. While electrical operation at substantially higher frequencies requires impedance matched electrodes for optimal performance, the high frequency limit can be estimated by the RC roll-off frequency $f_{RC} = (2\pi RC)^{-1}$ of the drive capacitor, where $R \sim 1\ \Omega$ is the resistance of the capacitor plate. Using the dimensions of the high-frequency cantilever shown in Fig. 2(e), we find C ~ 1.5 pF, which gives $f_{RC} >> 1$ GHz, so operation at GHz frequencies is attainable. Capacitive driving can also be used to drive higher order vibrational or torsional modes of the cantilever. The efficiency with which the driving force couples to a given mode is related to the positional overlap between the driving force and the deflection of the mode.[27] In our case, the capacitor covers the entire cantilever, thus the driving force is uniformly distributed. In the first resonance mode, the entire cantilever is moving in one

direction, so a uniform force drives the first mode efficiently. For higher modes or torsional modes, where the sign of the deflection varies along the cantilever, it is ideal to pattern the capacitor only in regions of deflection of a single sign, thus maximizing dot product between the driving force and displacement profile of the desired mode.

The authors thank Rafael Jaramillo, Katia Bertoldi, and Jason Cleveland for helpful discussions. We acknowledge support by the Department of Defense through a National Defense Science & Engineering Graduate (NDSEG) Fellowship and the Department of Energy through grant number DE-FG02- 07ER46422.

REFERENCES

[1]K. K. Leang and A. J. Fleming, in American Control Conference (2008) pp. 3188-3193.

[2]J. K. H. Hörber and M. J. Miles, Science **302**, 1002 (2003).

[3]M. Yokokawa, C. Wada, T. Ando, N. Sakai, A. Yagi, S. H. Yoshimura, and K. Takeyasu, EMBO J. **25**, 4567 (2006).

[4]D. C. Hurley, M. Kopycinska-Müller, A. B. Kos, and R. H. Geiss, Meas. Sci. Technol. **16**, 2167 (2005).

[5]M. Li, H. X. Tang, and M. L. Roukes, Nat. Nanotechnol. **2**, 114 (2007).

[6]J. L. Arlett, E. B. Myers, and M. L. Roukes, Nat. Nanotechnol. **6**, 203 (2011).

[7]D. Y. Abramovitch, S. B. Andersson, L. Y. Pao, and G. Schitter, in *American Control Conference* (2007) pp. 3488-3502.

[8]U. Rabe, S. Hirsenkorn, M. Reinstädtler, T. Sulzbach, C. Lehrer, and W. Arnold, Nanotechnology **18**, 044008 (2007).

[9]H. Yamashita, N. Kodera, A. Miyagi, T. Uchihashi, D. Yamamoto, and T. Ando, Rev. Sci. Instrum. **78**, 083702 (2007).

[10]K. I. Umeda, N. Oyabu, K. Kobayashi, Y. Hirata, K. Matsushige, and H. Yamada, Appl. Phys. Expr. **3**, 065205 (2010).

[11]S. C. Minne, S. R. Manalis, and C. F. Quate, Appl. Phys. Lett. **67**, 3918 (1995).

[12]K. Schwarz, U. Rabe, S. Hirsekorn, and W. Arnold, Appl. Phys. Lett. **92**, 183105 (2008).

[13]S. S. Chou, Y. Y. Kim, A. Srivastava, B. Murphy, O. Balogun, S.-H. Tark, G. Shekhawat,

and V. P. Dravid, Appl. Phys. Lett. **94**, 224103 (2009).

[14]G. Neubauer, S. R. Cohen, G. M. McClelland, D. Horne and C. M. Mate, Rev. Sci. Instrum. **61**, 2296 (1990).

[15]J. Brugger, N. Blanc, Ph. Renaud and N. F. de Rooij, Sensor Actuat. A-Phys. **43**, 339 (1994).

[16]S. Bouwstra, F. R. Blom, T. S. J. Lammerink, H. Yntema, P. Schrap, J. H. J. Fluitman and M. Elwenspoek, Sensor Actuator **17**, 219 (1989).

[17]Mechanical strain in the capacitor is found by treating the cantilever as a uniform isotropic Euler-Bernoulli beam[27] and including Poisson's effect. The films that make up the capacitor are thin and do not affect the mechanics.[28] The mechanical strain in the capacitor is assumed to be constant and equal to the strain on the surface of the cantilever.

[18]H. Y. Lee, Y. Peng, and Y. M. Shkel, J. Appl. Phys. **98**, 074104 (2005).

[19]D. Stryahilev, A. Sazonov, and A. Nathan, J. Vac. Sci. Technol. A **20**, 1087 (2002).

[20]M. P. Hughey and R. F. Cook, J. Appl. Phys. **97**, 114914 (2005).

[21]G. Hähner, J. Appl. Phys. **104**, 084902 (2008).

[22]K. A. Brown, J. A. Aguilar, and R. M. Westervelt, Appl. Phys. Lett. **96**, 123109 (2010).

[23]K. A. Brown, J. Berezovsky, and R. M. Westervelt, Appl. Phys. Lett. **98**, 183103 (2011).

[24]T. Fukuma, M. Kimura, K. Kobayashi, K. Matsushige, and H. Yamada, Rev. Sci. Instrum. **76**, 053704 (2005).

[25]To fit the amplitude noise spectra; the noise floor is attenuated to the 1-10 kHz level to remove high-frequency attenuation in the electronics. This leads to a 10% correction at 250 kHz and a 50% correction at 1.5 MHz.

[26]R. G. Beck, M. A. Eriksson, M. A. Topinka, R. M. Westervelt, K. D. Maranowski, and A. C. Gossard, Appl. Phys. Lett. **73**, 1149 (1998).

[27]S. S. Rao, Mechanical Vibrations, 3rd ed. (Addison-Wesley Publishing Company, Upper Saddle River, NJ, 1995).

[28]B. J. Rodriguez, S. Jesse, K. Seal, A. P. Baddorf, S. V. Kalinin, and P. D. Rack, Appl. Phys. Lett. **91**, 093130 (2007).

TABLE I. Properties of the conventional (1) and high-frequency (2) cantilevers used in this study. f_0 and k are found through fitting of n_A from Figs. 2(b) and 2(f), typical cantilever geometries are measured in a SEM, and D is estimated from ellipsometry of a test wafer.

	f_0	T	W	L	D	k	Q	α_{exp}	α_{theory}
	kHz	μm	μm	μm	nm	nN/nm		nm/V^2	nm/V^2
1	243	4.6	57	163	68	47	487±22	0.62	0.9
2	1526	0.4	37	33	50	2.7	188±5	0.78	1.5

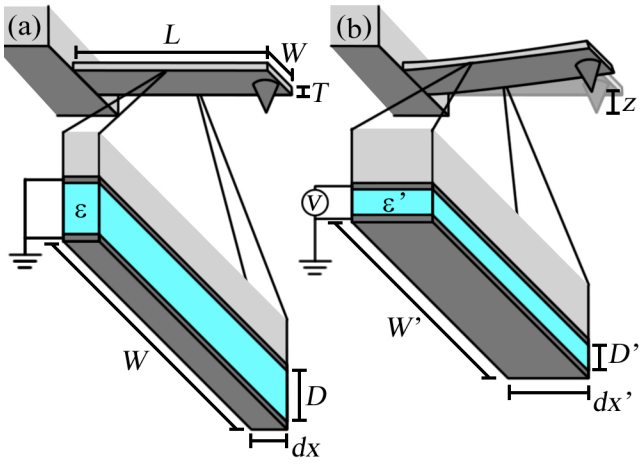

FIG. 1. (a) Schematic of a cantilever with a thin-film capacitor on its bottom face. (b) The application of a voltage across the capacitor causes a deflection that changes the dimensions and dielectric properties of the capacitor.

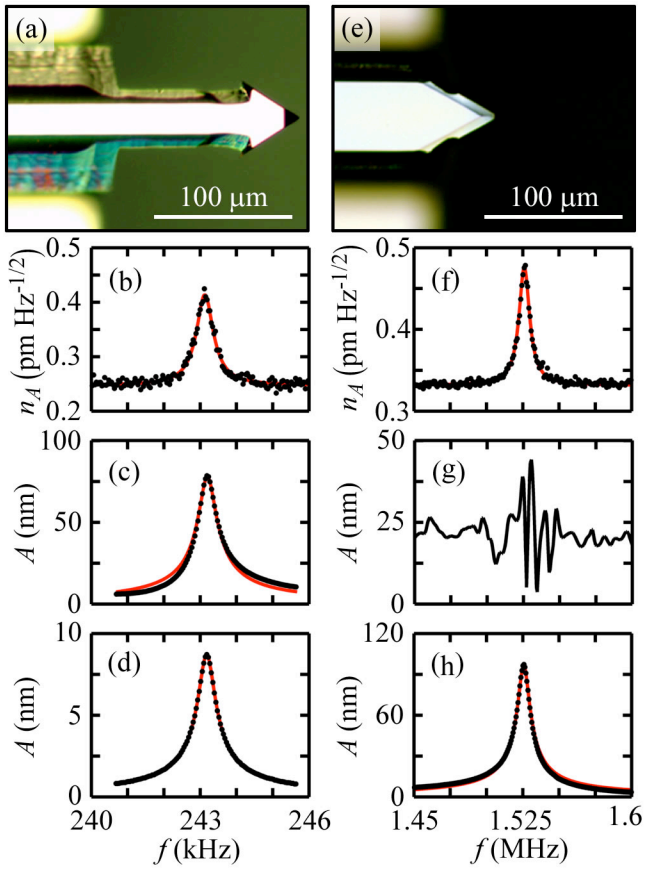

FIG. 2. Comparison of mechanical and capacitive driving of the first mechanical resonance mode for a conventional tapping-mode (left column) and a high-frequency (right column) cantilever. Points are experimental data and lines are fits of the data to theory. (a,e) Optical images of the tapping mode and high-frequency AFM probes after fabrication. (b,f) Thermal amplitude spectra n_A *vs.* frequency f showing the first mechanical resonance peak. (c,g) Cantilever vibration amplitude A *vs.* f when the probe is driven by mechanically shaking it with the piezoelectric element. (c) The frequency dependant transfer function between the actuator and the cantilever creates only a small deviation from the theoretical fit for the tapping mode cantilever but (g) mixing with unwanted mechanical modes of the drive system makes the resonance unintelligible for the high-frequency cantilever. (d,h) When driven capacitively, the measured response A *vs.* f is in excellent agreement with theory, demonstrating the advantage of high-fidelity capacitive drive.

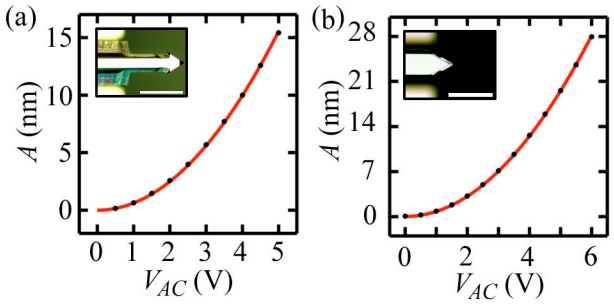

FIG. 3. Cantilever vibration amplitude A for (a) tapping-mode and (b) high-frequency AFM cantilevers driven capacitively using an ac-voltage V_{AC} at half the resonant frequency $f = f_0/2$.. The experimental data points are fit very well by $A = \alpha_{exp} V_{AC}^2$, shown by the line. The insets show optical images of each cantilever with a 100 μm scale bar.